Universiteit
Leiden
The Netherlands

# Pharmacokinetic and pharmacodynamic analysis in anesthesia : a modeling odyssey

Olofsen, E.

**Citation**
Olofsen, E. (2017, June 21). *Pharmacokinetic and pharmacodynamic analysis in anesthesia : a modeling odyssey*. Retrieved from https://hdl.handle.net/1887/50818

| | |
|---|---|
| Version: | Not Applicable (or Unknown) |
| License: | Licence agreement concerning inclusion of doctoral thesis in the Institutional Repository of the University of Leiden |
| Downloaded from: | https://hdl.handle.net/1887/50818 |

**Note:** To cite this publication please use the final published version (if applicable).

Cover Page

Universiteit Leiden


The handle http://hdl.handle.net/1887/50818 holds various files of this Leiden University dissertation

**Author**: Olofsen, E.
**Title**: Pharmacokinetic and pharmacodynamic analysis in anesthesia : a modeling odyssey
**Issue Date**: 2017-06-21

# Chapter 5

# Population Analysis of Kalman-Filtered Permutation Entropy of the Electroencephalogram*

General anesthetics produce dose-dependent effects on the electroencephalogram (EEG), causing an increase in power combined with a decrease in average EEG frequency.[62] A novel EEG-derived parameter is the permutation entropy (PE) of the EEG.[65] Important advantages are its robustness under eye blinks, and its ease of computation. The permutation entropy quantifies the probability distribution of motifs present in the signal, and it is determined by the dominant frequency in the EEG signal. But because of the ordinal (counting) nature of the PE, it is dominated by the presence of high EEG frequencies, even if they have quite small amplitudes.

Anesthetic concentration-effect data fits often show systematic misfits, due to correlated residuals, which could lead to biased standard errors of parameter estimates and false conclusions from statistical tests. Kalman filters may be constructed to separate measurement and process noise.[43,90] The first objective of the present study was to construct a pharmacokinetic-pharmacodynamic (PK-PD) model, including a Kalman filter, to analyze concentration-permutation entropy data sets. The second objective was to gain more insight into the effects of the incorporation of a Kalman filter, by fitting models with and without a Kalman filter to simulated data.

## 5.1 Methods

### 5.1.1 Ordinal Statistics and the Calculation of the Permutation Entropy

With the possible exception of zero-crossing rate, most EEG indices use the EEG signal as a continuously variable signal (to the limits of the measuring equipment). In contrast, ordinal statistics rank the data from smallest to largest, and then compare the rankings. Therefore, the use of ordinal descriptions of EEG may have the advantage of being re-

* Parts have been published in E Olofsen, J W Sleigh, A Dahan, *Br J Anaesth* 2008; 101:810–821, 2008, and E Olofsen, *PAGE* 2011: Abstract #2202

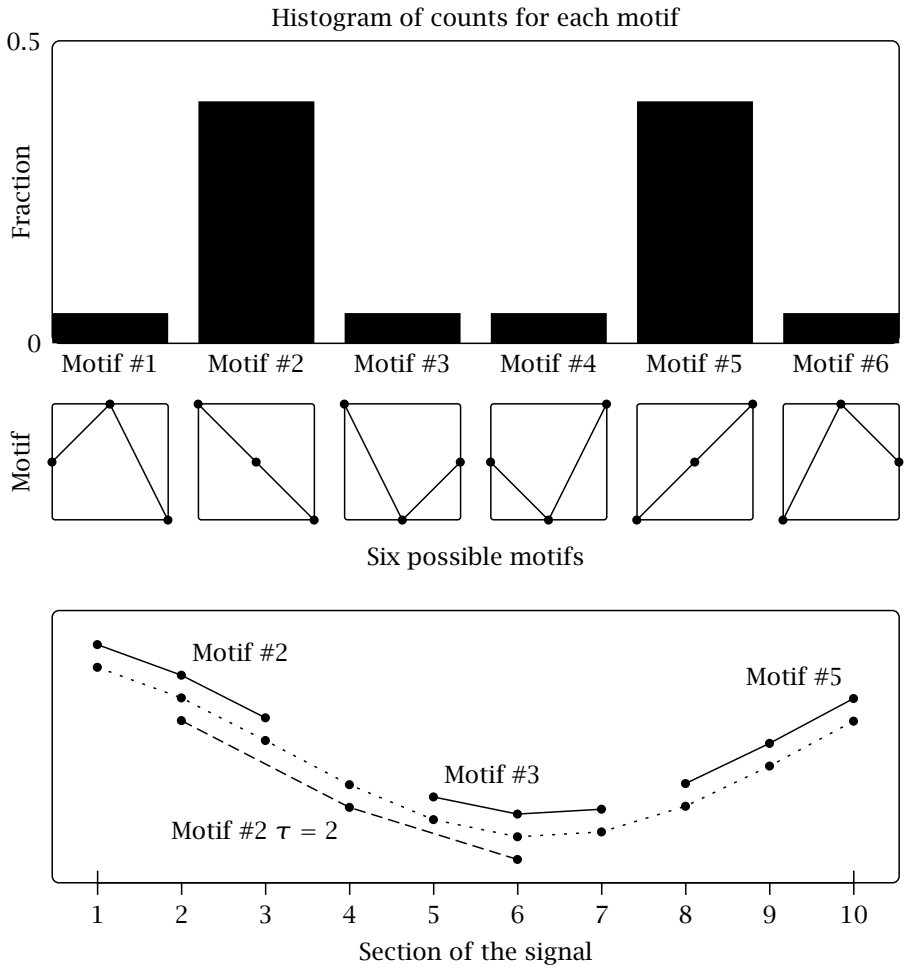


**Figure 5.1: Lower panel**: extraction of ordinal patterns from the EEG signal. As the algorithm moves sequentially through the EEG signal, the sections ("motifs" consisting of three data points' length) are classified as one of the six possible patterns, depicted in the middle panel. **Upper panel**: a histogram of the relative numbers of each motif in the signal. The dashed-line motif is a demonstration of the operation of the $\tau = 2$ lag.

sistant to large artifacts that occur with low frequencies. In this article, we will refer to the elemental patterns that are extracted from the EEG signal as "motifs" (see Figure 5.1 for graphical explanation). The EEG signal can therefore be considered to consist of a sequence of ordinal motifs.

The use of PE to quantify EEG changes in seizures was originally proposed by Bandt and Pompe,[8] and this work has been further developed by Cao and colleagues.[20] The algorithm of the calculation of the PE is quite simple and is depicted diagrammatically in Figure 1 as follows:

1. Fragment the continuous EEG signal (dotted line in the lower diagram of Figure 5.1), into a sequence of motifs (some examples are shown above and below the signal);

2. Identify each motif as belonging to one of the six possible types (as shown as 6 diagrams in the middle panel in Figure 5.1) - according to their shape [we describe

the six types as two varieties each of "slopes" (motifs #2 and #5 in Figure 5.1), "peaks" (motifs #1 and #6), and "troughs" (motifs #3 and #4)];

3. Count the number of motifs of each of the six categories, to obtain the probability of occurrence of each motif in the signal ($p_i$) (upper diagram in Figure 5.1);

4. Calculate the PE of the resultant normalized probability distribution of the motifs, using the standard Shannon uncertainty formula:[76]

$$\mathrm{PE} = -\frac{\Sigma p_i \cdot \log(p_i)}{\log(\text{number of motifs})} \tag{5.1}$$

Thus, the PE is a way of quantifying the relative occurrence of the different motifs. Like other entropies, the PE is simply a measure of the "spread-outness", or "flatness", or "uncertainty" in the frequency distribution. When the EEG signal is dominated by high frequencies, there will be almost equal numbers of each species of motif in each EEG segment analyzed. The properly normalized entropy is maximal (PE=1.0), if there is an equal distribution of motifs between each of the six patterns. Conversely, when the signal consists of slow delta waves, there will be relatively more of the "slope" motifs (motifs #2 and #5 in Figure 5.1), and fewer of the other "peak" and "trough" motifs, and the entropy decreases. The PE of a signal consisting of a single motif (such as one very long "up-slope") is zero. However, the effective realistic minimum value of the PE is about 0.4. It is important to note that the PE is very different from the spectral entropy in its frequency response. The PE tends to decrease as the frequency decreases Figure 5.2), whereas the value of the spectral entropy is completely independent of frequency *per se*, but only measures the sharpness of the frequency peak. To test the responses of the various PEs to variations in frequency, artificial "pseudo-EEG" signals were generated, using a C++ computer program which allowed known amounts of white noise to be added to various pure sine wave frequencies (Figure 5.2).

In summary, the PE quantifies the probability distribution of motifs present in the signal, and is determined both by the dominant frequency in the EEG signal and by the bandwidth. Because of the ordinal (counting) nature of the PE, this is dominated by the presence of higher EEG frequencies, even if they have quite small amplitudes.

### 5.1.2 Parameters and Ties

The PE has two predefined parameters. (i) The "order" of the PE is the number of data points that are included in each motif. We restricted our study to include only short motifs of just three points (order=3). Exploratory data analysis suggested that the use of longer motifs did not contribute to a better index of depth of anesthesia. (ii) The "lag" ($\tau$) of the PE is the number of sample points spanned by each section of the motif. In the lower diagram in Figure 1, the dark grey motifs are of lag $\tau = 1$, because they are made up of adjacent data points. The longer light grey motif is of lag $\tau = 2$, because the length of each section of the motif is two data points. The importance of the lag is that it gives the resultant PE different frequency characteristics (Figure 5.2). Most of the anesthetic-related information in the EEG can be extracted using a lag ($\tau = 1$) of one sample step (assuming a sampling frequency of about 128 $s^{-1}$). However, as described in our earlier paper,[65] the inclusion of lag ($\tau = 2$) helped differentiate deeper planes of anesthesia, and resulted in better PK-PD modeling.

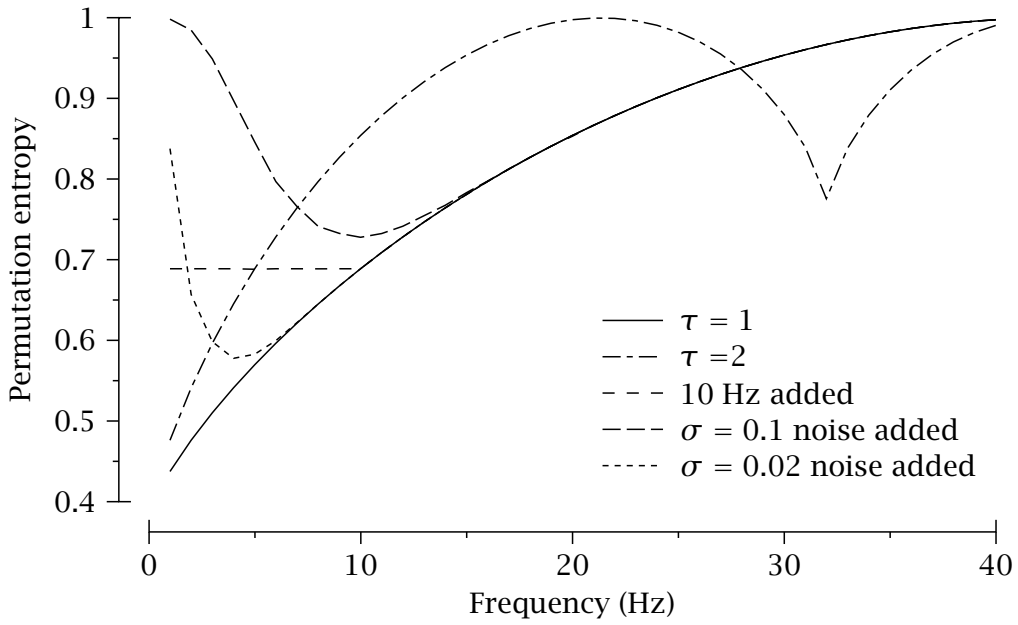


**Figure 5.2:** The frequency dependence of the permutation entropy with different lags ($\tau = 1$ and $\tau = 2$), and response to added white noise or a second sine wave oscillation. Long signals (65536 samples) were used to minimize fluctuations.

It is possible that two (or indeed all three) of the data points in a motif may have the same measured voltage because of the limited resolution of the analogue-digital conversion, and therefore are not able to be ranked. Although this occurrence may seem to be very unlikely, it raises the important issue of how to deal sensibly with very small voltage fluctuations in the EEG. A flat-line EEG indicates an almost absolutely quiescent cerebral cortex. If we have a high-resolution analogue-to-digital converter, the PE will continue to estimate the minute fluctuations in the signal - and its value typically increases. Unfortunately, these fluctuations are made up largely of various types of measurement noise, and are not reflecting drug actions on the cerebral cortex. This is most apparent when the burst suppression EEG pattern is present during deep anesthesia. One solution is to arbitrarily assign a third parameter - the threshold level, below which, most of the "signal" is thought to consist of noise. In our earlier paper, we chose the value of 0.5 $\mu$V as a threshold level. If the difference between any two of the points in the motif is below the threshold, then the motif was counted as a seventh category of "motif" - a "tie". However, for simplicity with regard to computations and analysis, in the remainder of this chapter the standard PE (with $m = 3$, $\tau = 1$) was used.

### 5.1.3 Application to Real EEG signals

Fourteen raw EEG data sets (from 7 male and 7 female patients; an extension of the data described in an earlier publication[62]) without burst suppression were analyzed using the population analysis approach. Step-wise changes in end-tidal isoflurane concentration were applied. The pharmacokinetic part of the PK-PD describes the relationship between the end-tidal and brain or effect-site concentration. The pharmacodynamic part of the model describes the relationship between the brain concentration and the measured

effect. It was assumed that this relationship is nonlinear, monotonically decreasing and can be described by the inhibitory sigmoid-$E_{\max}$ model with steepness parameter $\gamma$.

Previously,[62] we performed a two-stage analysis, *i.e.*, the data were fitted for each subject separately and next the obtained parameter values were averaged. In the present chapter, first both a two-stage and population analysis were performed to assess the importance of differences between the methods. Next, a population analysis of permutation entropy data based on the same EEGs was performed to assess the performance of permutation entropy *versus* BIS. An extended Kalman filter was constructed to analyze permutation entropy data. This was motivated by the fact that many data fits show systematic misfits; this may lead to biased standard errors of parameter estimates and false conclusions from statistical tests. Finally, simulations were performed to study the effects of the incorporation of a Kalman filter by fitting models with and without a Kalman filter to simulated data.

The Kalman filter is a method to track the state of a system in the presence of measurement and system noise. The extended Kalman filter is a generalization for linearized nonlinear systems. Tornøe *et al.* described[90] its implementation in the statistical analysis package NONMEM.[9] The Kalman filter state and functions of the state need to be defined to describe how the state evolves in time, how it is affected by an input, and how it propagates to the output. Two versions were constructed. Version A assumes that colored noise is present on the model output, albeit limited by maximum and minimum values of PE. Version B assumes that noise enters the system at the input, so at the level of anesthetic concentration. Because the process noise term is assumed to be normally distributed, it was added to the logarithm of concentration. NONMEM version 7 was used for parameter estimation. The differential equations describing the effect-site concentration, the Kalman filter state, and its variance were implemented as one (recursive) difference equation. The Kalman filter gain could be solved from the estimates of the measurement and process noise variances and hence needed no recursive approximation. The initial filter state was a parameter to be estimated, in addition to the parameters of the PK-PD model. The model incorporating Kalman filter version B was used to generate 1000 sets of artificial data of 10, 20, 50 and 100 individuals, with parameter values from the final model of the permutation entropy data. These data were fitted by the same model to check that parameter estimation was consistent, and by the model without Kalman filter.

### 5.1.4 PK-PD Modeling

The anesthetic concentration-effect data were analyzed with the pharmacodynamic model as described earlier.[62] Briefly, the pharmacodynamic model consisted of a hypothetical effect compartment combined with a sigmoid-$E_{\max}$ model described by the equations

$$\frac{dC_e(t)}{dt} = k_{e0} \cdot (F_{ET}(t) - C_e(t)) \tag{5.2}$$

and

$$E(t) = E_{\max} + (E_{\min} - E_{\max}) \cdot \frac{C_e(t)}{C_e(t) + \mathrm{IC}_{50}^{\gamma}}, \tag{5.3}$$

where $F_{ET}(t)$ is end-tidal isoflurane concentration; $k_{e0}$ the rate constant determining the speed of equilibrium (we estimated the effect-site equilibration half-time $t_{½,k_{e0}}$), $C_e(t)$

is the effect-site concentration, $E(t)$ is the effect measure (permutation entropy or BIS), $E_{\max}$ and $E_{\min}$ are the maximal and minimal values of $E$, $IC_{50}$ is the concentration that places $E$ halfway between $E_{\min}$ and $E_{\max}$, and $\gamma$ is a steepness parameter. In the mixed-effects analysis, all parameters were assumed to be lognormally distributed, and that residual error was normally distributed. Parameters $E_{\max}$ and $E_{\min}$ were constrained to the interval (0,1) and $\gamma$ to the interval (0,25) *via* the inverse logit transform.

### 5.1.5 Two Extended Kalman Filters

Kalman filter A assumes that colored noise is present on the model output, albeit limited by $E_{\max}$ and $E_{\min}$. With

$$\gamma(t) = \log\left(\frac{1 - E(t)}{E(t)}\right),$$

where $E(t)$ is given by equation (5.3), and

$$\frac{dx}{dt} = g(x) + \nu = -\frac{x(t)}{\tau} + \nu,$$

where $x$ is the state of the system and $\nu$ is system noise (a Wiener process[67]), the output is given by

$$E'(t) = \frac{1}{1 + \exp(x + \gamma)} + \epsilon$$

So $E'(t)$ resembles $E(t)$, but contains colored noise, filtered by time constant $\tau$, and is, without the noise term, still constrained to the interval (0,1). Note that while we retain the notation with $\tau$, this parameter is different from the lag used to calculate the permutation entropy.

Kalman filter B assumes that process noise enters the system at the input, so at the level of anesthetic concentration. Because the noise term $\nu$ has to be normally distributed, it was added to the logarithm of concentration, and then the system state is

$$\frac{dx}{dt} = g(x) + \nu = \frac{1}{\tau}\left(\gamma \cdot \log\left(\frac{C_{ET}(t) + C_{ET,0}}{IC_{50}}\right) - x\right) + \nu \tag{5.4}$$

and the output is given by

$$E'(t) = E_{\min} + \frac{1 - E_{\min}}{1 + \exp(x)} + \epsilon, \tag{5.5}$$

where $C_{ET,0}$ a parameter that yields finite values of the logarithm and replaces $E_{\max}$. The time delay is determined by several factors.[62] By placing the system noise at the level of concentration, $\tau$ may be viewed as neural processing rather than blood–brain concentration equilibration delay ($t_{½,k_{e0}}$).

For both versions, the derivative of $g(x)$ with respect to $x$ is $-1/\tau$. This implies that the differential equation for the variance $P$ of $x$ is

$$\frac{dP}{dt} = -\frac{2P}{\tau} + \sigma_w^2.$$

Both $x$ and $P$ were solved for discrete time steps $\Delta t$ under the assumption that the

input changes step-wise. For example, the next $P_{i+1}$ is given by

$$P_{i+1} = P_i \cdot \exp\left(-\frac{2\Delta t}{\tau}\right) + \frac{\tau\sigma_w^2}{2}\left(1 - \exp(-\frac{2\Delta t}{\tau})\right).$$

In this way, the differential equations described here are transformed to difference equations, which can be solved by NONMEM, without the need for special compartment reset records in the input file as described by Tornøe *et al.*[90] The Kalman gain of the extended Kalman filter depends on the derivative of $E'(t)$ with respect to $x$, and was computed as given by Tornøe *et al.*[90]

### 5.1.6 Simulation Study

The model incorporating Kalman filter version B was used to generate 1000 sets of artificial data of 100 individuals, with parameter values from the final model of the permutation entropy data. The individual data consisted of 241 data points (time between 0 and 60 min, $\Delta t$ 0.25 min). These data were fitted by the same model to check that the parameter estimation is consistent, and by the model without Kalman filter to study its effects on parameter estimates.

## 5.2 Results

### 5.2.1 Application to Real EEG signals

#### Two-Stage *versus* Population Analysis

Table 5.1 presents the results from the two-stage and population analyses of the BIS data. The population analysis provides estimates of the parameters, and of their variability across the population. The parameter estimates are similar, and interestingly, the SEMs of the two-stage analysis and standard errors from the population analysis also agree. On the other hand, the squares of the standard deviations from the two-stage analysis do not correspond to the inter-individual variance. These two results are due to the fact that interindividual variability is relatively small compared to parameter uncertainties in each individual (residual intraindividual variance was $50.4 \pm 6.23$), despite the number of observations per individual ($\approx 200$). Model fits are shown in the top panels of Figure 5.3. Worst, median and best fits were selected based on the coefficient of determination ($R^2$ $\approx 0.79$, 0.92, and 0.98 for IDs 24, 12, and 18 respectively). The bottom panels show the applied (as measured) end-tidal isoflurane concentration.

#### Bispectral Index *versus* Permutation Entropy

Table 5.2 presents the results from population analysis of the permutation entropy data. Apart from obvious differences with the results for the BIS between $E_{\max}$ and $E_{\min}$ the much larger interindividual variability of $\gamma$ is notable. This is related to the occurrence of some rather high values of $\gamma$ - see the steep fall in PE in Figure 5.3 for ID 12 ($\gamma \approx 18$). This, in turn, may be related to the occurrence of high-frequency EEG activity, falsely (or not) increasing the measure of depth of anesthesia.

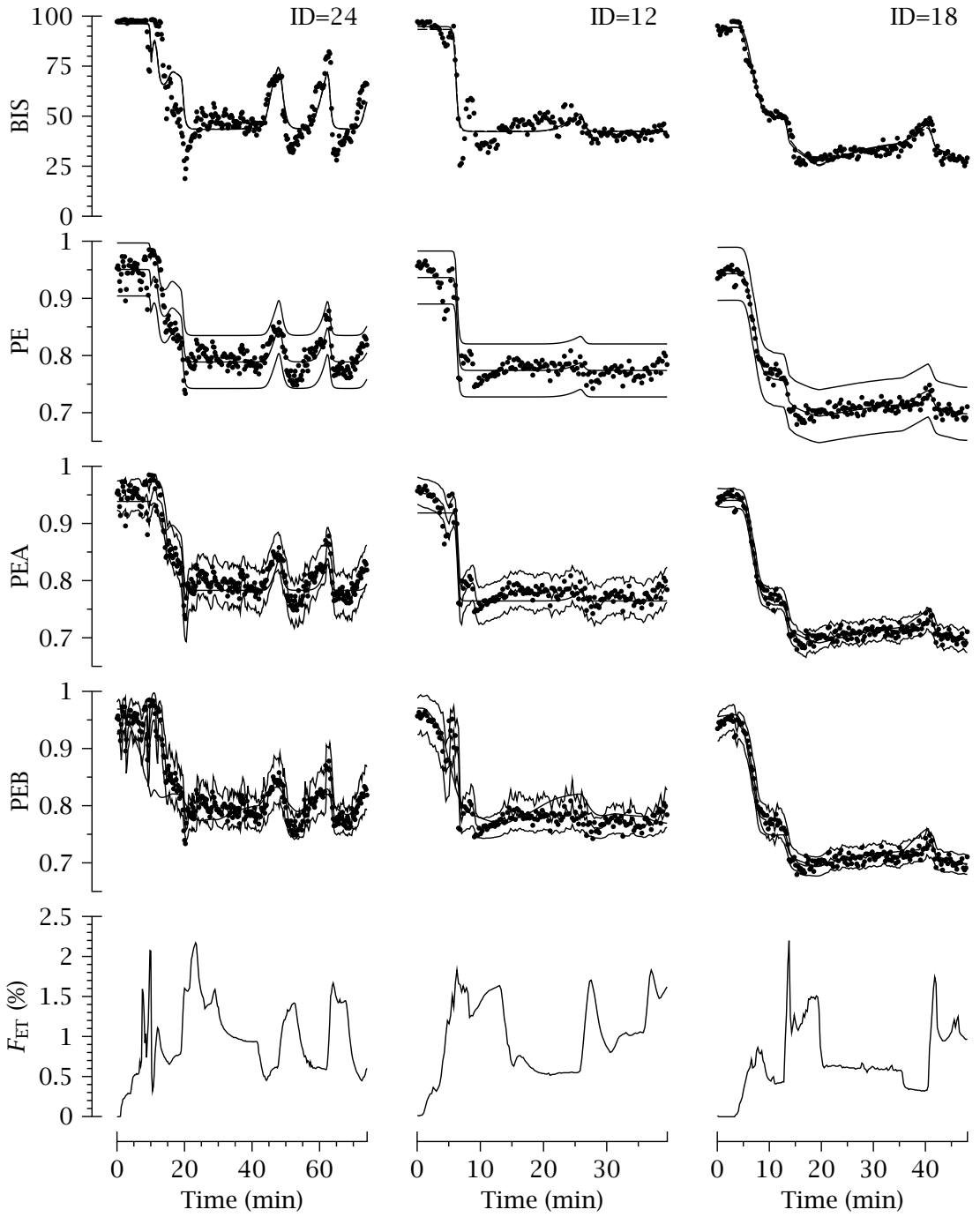


**Figure 5.3:** Administered isoflurane concentration ($F_{ET}$, bottom panels), BIS and permutation entropy data with fits (median ± 95% CI) without Kalman filter (PE), Kalman filter A (PEA), and Kalman filter B (PEB), for three subjects.

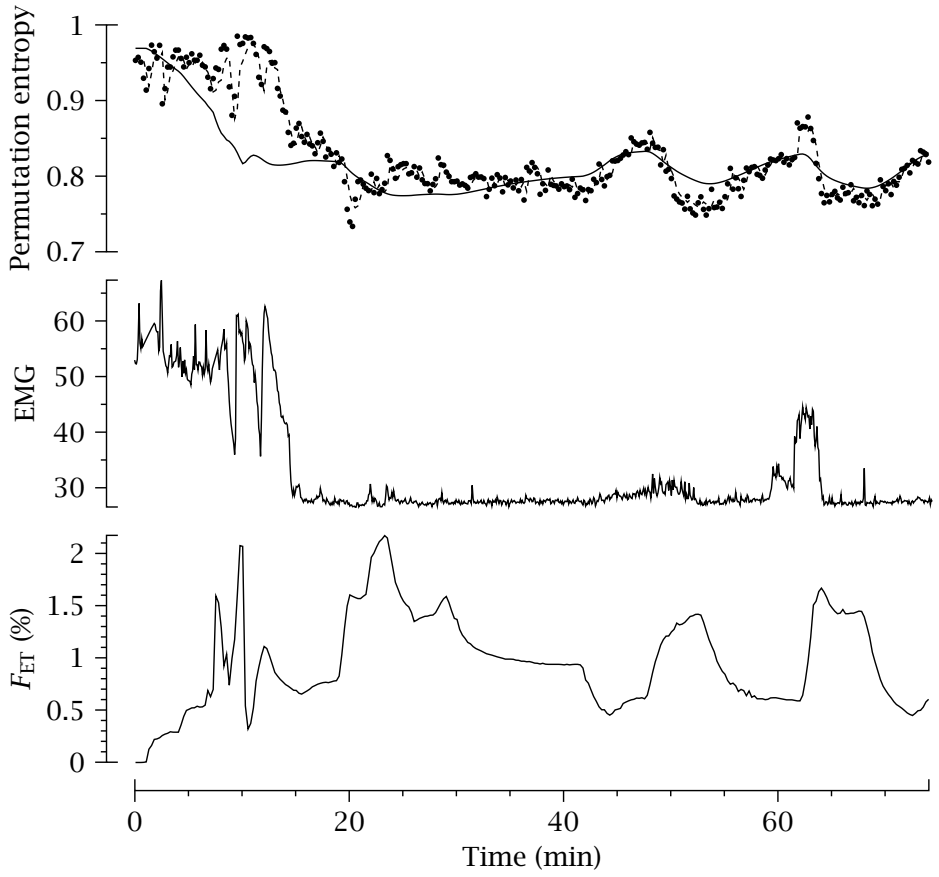


**Figure 5.4:** **Upper panel**: Close-up of the permutation entropy data fit of Subject 24. The dashed line is the Kalman-filtered permutation entropy; the solid line is the model prediction if there were no process noise. **Middle panel**: Electromyographic activity (EMG). **Lower panel**: Administered isoflurane concentration ($F_{ET}$).

**Table 5.1:** Parameter estimates from the Two-Stage and Population Analyses of the BIS data.

| | Two-Stage Analysis | | | Population Analysis | | | |
|---|---|---|---|---|---|---|---|
| Parameter | Est. | SD | SEM | Est. | SE | $\omega^2$ | SE |
| $t_{½,k_{e0}}$ (min) | 4.24 | 1.20 | 0.321 | 4.06 | 0.309 | 0.0744 | 0.0175 |
| $\gamma$ | 5.94 | 4.14 | 1.11 | 5.05 | 0.831 | 0.508 | 0.255 |
| $IC_{50}$ (%) | 0.575 | 0.107 | 0.0286 | 0.558 | 0.0302 | 0.0412 | 0.0182 |
| $E_{max}$ | 95.9 | 1.86 | 0.497 | 95.8 | 0.508 | 0.0945 | 0.0443 |
| $E_{min}$ | 27.2 | 10.8 | 2.87 | 27.4 | 2.55 | 0.199 | 0.0907 |

SEM is SD divided by the square root of the number of subjects.

**Table 5.2:** Population Analysis of the PE Data (without Kalman filter).

| Parameter | Est. | SE | $\omega^2$ | SE |
|---|---|---|---|---|
| $t_{½,k_{e0}}$ | 4.37 | 0.350 | 0.0803 | 0.0235 |
| $\gamma$ | 6.79 | 2.52 | 2.27 | 1.63 |
| $IC_{50}$ | 0.506 | 0.0408 | 0.0633 | 0.0336 |
| $E_{max}$ | 0.947 | 0.00296 | 0.0386 | 0.0145 |
| $E_{min}$ | 0.727 | 0.00827 | 0.0238 | 0.00991 |

See Methods section for explanation of parameters.

**Table 5.3:** Population Analysis of the PE Data with Kalman Filter A.

| Parameter | Est. | SE | $\omega^2$ | SE |
|---|---|---|---|---|
| $t_{½,k_{e0}}$ | 4.28 | 0.450 | 0.129 | 0.0328 |
| $\gamma$ | 17.2 | 5.18 | 9.49 | 4.45 |
| $IC_{50}$ | 0.501 | 0.0393 | 0.0785 | 0.0415 |
| $E_{max}$ | 0.937 | 0.00617 | 0.0636 | 0.0894 |
| $E_{min}$ | 0.729 | 0.0111 | 0.0314 | 0.0121 |
| $\tau$ | 5.41 | 1.13 | - | - |
| $\sigma_m$ | 0.0113 | 0.000666 | 0.0326 | 0.0137 |
| $\sigma_s$ | 0.102 | 0.0123 | 0.221 | 0.136 |
| $x_0$ | -0.344 | 0.208 | 0.260 | 0.287 |

$\sigma_m$ and $\sigma_s$ are the standard deviations of the measurement and process noise sources, respectively.
$x_0$ is the initial state of the system.
A dash indicates that the $\omega^2$ was not estimable.

### Kalman-Filtered Permutation Entropy

Table 5.3 and Figure 5.3 (PEA panels) present the results from population analysis of the permutation entropy data with Kalman filter A. Unfortunately, the estimate of $\gamma$ and its interindividual variance increased (for ID 12 to $\approx$ 24, while it was limited to 25). It is unfortunate, because it means that the PE as a candidate measure of depth of anesthesia reduces to an on/off indicator.

Table 5.4 presents the results from population analysis of the permutation entropy data with Kalman filter B. Now, the estimate of $\gamma$ and its interindividual variance decreased to a useful value. In Figure 5.3 it can be seen that PEB is still sensitive to higher isoflurane concentrations instead of being saturated. Moreover, note that all interindividual variabilities are smaller than those obtained from the analysis without Kalman filter (although we do not know the right values - see next subsection using simulated data). Figure 5.4 shows a close-up of the analysis for ID 24. High-frequency EEG activity and/or EMG activity elevates the PE. The Kalman-filtered PE seems to filter out this activity. See also the EMG activity at about 60-65 minutes.

A bootstrap analysis has been proposed to validate the parameter estimates.[30] Furthermore, the method can be used to obtain 95% confidence intervals. Results from the

**Table 5.4:** Population Analysis of the PE Data with Kalman Filter B.

| Parameter | Est. | SE | $\omega^2$ | SE |
|---|---|---|---|---|
| $t_{½,k_{e0}}$ | 3.50 | 0.248 | - | - |
| $\gamma$ | 2.60 | 0.677 | 0.0355 | 0.0204 |
| $IC_{50}$ | 0.635 | 0.191 | 0.0210 | 0.0114 |
| $C_{ET,0}$ | 0.280 | 0.163 | - | - |
| $E_{min}$ | 0.699 | 0.00832 | 0.0165 | 0.00726 |
| $\sigma_m$ | 0.00837 | 0.000286 | - | - |
| $\sigma_s$ | 0.516 | 0.0398 | 0.0766 | 0.0384 |
| $x_0$ | 0.499 | 0.320 | - | - |

$C_{ET,0}$ is a parameter related to $E_{max}$ (see Methods).

**Table 5.5:** Bootstrap Analysis of the PE Data with Kalman Filter B.

| Parameter | Est. | SE | 95% CI | $\omega^2$ | SE | 95% CI |
|---|---|---|---|---|---|---|
| $t_{½,k_{e0}}$ | 3.50 | 0.241 | 3.07-3.97 | | | |
| $\gamma$ | 2.77 | 0.823 | 1.73-4.79 | 0.0333 | 0.0252 | 0.00343-0.0909 |
| $IC_{50}$ | 0.679 | 0.225 | 0.392-1.23 | 0.0179 | 0.0129 | 0.00181-0.0430 |
| $C_{ET,0}$ | 0.322 | 0.198 | 0.104-0.831 | | | |
| $E_{min}$ | 0.700 | 0.00787 | 0.684-0.716 | 0.0150 | 0.00681 | 0.00223-0.0281 |
| $\sigma_m$ | 0.000839 | 0.000285 | 0.00787-0.00895 | | | |
| $\sigma_s$ | 0.516 | 0.0436 | 0.435-0.600 | 0.0724 | 0.0384 | 0.0157-0.157 |
| $x_0$ | 0.554 | 0.289 | 0.0767-1.21 | | | |

bootstrap are given in Table 5.5. A comparison with the results in Table 5.4 shows that all estimates, including the standard errors, are similar. Unfortunately, the estimate of $IC_{50}$ is rather imprecise; without the Kalman filter it was much more precise. Of course, at this stage it is unknown which precision estimate is the most useful; the more precise $IC_{50}$ may be related to the description of the presence or absence of EMG activity rather than EEG activity.

### 5.2.2 Simulation Study

One thousand simulated data were generated using the model with Kalman filter B and parameter values listed in Table 5.4. These data were fitted with the same model, without and with Kalman filter, the results of which are presented in Table 5.6 and Table 5.7, respectively. The standard deviations from the 1000 estimates were calculated and the medians of the 1000 estimates of the standard errors (actually only NONMEM's succesful estimation and covariance runs were used ($\approx$ 930)). The medians were used because the estimates of the standard errors in the analyses with Kalman filter sometimes had quite large values; and also without the Kalman filter these are approximately lognormally distributed.

Without the Kalman filter, the median(SE) were somewhat less than the SDs (the

**Table 5.6:** Population Analysis of simulated data without Kalman filter.

| Parameter | Est. | SD | median(SE) | $\omega^2$ | SD | median(SE) |
|---|---|---|---|---|---|---|
| $t_{½,k_{e0}}$ | 3.71 | 0.234 | 0.215 | 0.288 | 0.0675 | 0.0554 |
| $\gamma$ | 2.67 | 0.222 | 0.211 | 0.625 | 0.149 | 0.133 |
| $IC_{50}$ | 0.531 | 0.0186 | 0.0173 | 0.0821 | 0.0207 | 0.0184 |
| $E_{max}$ | 0.961 | 0.00218 | 0.00213 | 0.296 | 0.0438 | 0.0430 |
| $E_{min}$ | 0.697 | 0.00632 | 0.00600 | 0.0562 | 0.0136 | 0.0118 |

**Table 5.7:** Population Analysis of simulated data with Kalman filter.

| Parameter | Est. | SD | median(SE) | $\omega^2$ | SD | median(SE) |
|---|---|---|---|---|---|---|
| $t_{½,k_{e0}}$ | 3.46 | 0.0914 | 0.0927 | - | - | - |
| $\gamma$ | 2.49 | 0.181 | 0.184 | 0.0328 | 0.00663 | 0.00642 |
| $IC_{50}$ | 0.622 | 0.0514 | 0.0506 | 0.0218 | 0.00502 | 0.00499 |
| $C_{ET,0}$ | 0.270 | 0.0392 | 0.0395 | - | - | - |
| $E_{min}$ | 0.699 | 0.00292 | 0.00282 | 0.0164 | 0.00247 | 0.00239 |
| $\sigma_m$ | 0.00853 | 0.0000743 | 0.0000759 | - | - | - |
| $\sigma_s$ | 0.480 | 0.0140 | 0.0145 | 0.0730 | 0.0124 | 0.0122 |
| $x_0$ | 0.442 | 0.0650 | 0.0638 | - | - | - |

means were also somewhat smaller (data not shown)). This may be related to the fact that residuals are correlated if the Kalman filter is not applied. More importantly, the estimates of interindividual variability are too large, for example for $t_{½,k_{e0}}$, where it was actually zero, or for $\gamma$ where the estimates differ a factor of 20. The $IC_{50}$ was set at 0.635; the estimate of $0.531 \pm 0.0186$ is clearly biased.

## 5.3 Discussion

Ordinal measures of EEG patterns have very different characteristics to traditional methods that use the raw EEG signal. The conceptual difference may be summed up in the phrases: not “how large is the pattern?” but rather “how many patterns exist?”.[65] Our preliminary investigations[65] indicated that the permutation entropy shows promise as a practical EEG measure of GABAergic hypnotic drug effect. It appropriately tracks the qualitative assessment of the EEG pattern from awake to sedated/lightly anesthetized, and to deeply anesthetized. It requires minimal preprocessing and is very resistant to blink artifacts.

A wide variety of other EEG indices have been used in PK-PD modeling.[65] At the present time, the most commonly used are the commercial ones (*e.g.*, BIS). Most indices require extensive and sophisticated artifact handling to achieve acceptable results, and this always runs the risk of distorting the EEG signal. The resistance to blink artifacts (and speed of computation) is a big advantage of the PE over other indices, producing stable values in the pre- and early induction period. The PE is comparable with the BIS in the spread of values between patients before and after loss-of-consciousness. Our

present results indicate that the PK-PD models that may be constructed using the PE are as acceptable as those constructed using the BIS.

A characteristic feature of the state of general anesthesia is the presence of large slow fluctuations in the instantaneous frequency content of the EEG. The most extreme example of this phenomenon is the burst suppression pattern, which needs special precautions,[65] so for the present analyses only data without burst suppression were used.

As for all EEG monitors, the PE is effectively computed from an EEG signal which is inextricably linked with the frontalis EMG. The same reason that makes the PE stable during the awake state also makes it very sensitive to episodic high-frequency fluctuations (artifactual, electromyographical, and neurophysiological) during deep anesthesia (see Figures 5.2 and 5.4 for illustration).

So while the PE is insensitive to eye blinks, it is sensitive to high frequency components present in the EEG just before loss of consciousness. This causes EEG effect parameters to respond relatively late and suddenly to a change from wakefulness into anesthesia. This property also results in a steep concentration-effect relationship. Analysis of EEG data with a Kalman filter accentuated or filtered out this phenomenon, depending on the postulated location of process noise. Version B provided a more useful pharmacodynamic model, because version A with the steep concentration-effect relationship impedes timely prediction of (sudden) awakening. Furthermore, the large steepness may, at least partly, be based on a confounding effect or artifact. It should be noted that this artifact filtering is only possible if the anesthetic concentration is known. The main difference between the two applied Kalman filters lies in the location of the process noise, *i.e.*, before or after the sigmoid-$E_{\max}$ concentration-effect relationship. Process noise may substitute for model inadequacies, in this case an EEG effect which was (in the model) not related to anesthetic concentration. So the confounding effect may need to be scaled, due to nonlinearities, to the level of the real process noise.

Finally and most importantly, the simulation study showed that if Kalman filtering is not applied, inter-individual variability may be overestimated; variability that is actually intra-individual process noise.